



Cite this: DOI: 10.1039/c8cc03218a

 Received 27th April 2018,
Accepted 24th May 2018

DOI: 10.1039/c8cc03218a

rsc.li/chemcomm

Design of functionalized cyclic peptides through orthogonal click reactions for cell culture and targeting applications†

 Paige J. LeValley,[‡] Elisa M. Ovadia,[‡] Christopher A. Bresette,^a Lisa A. Sawicki,^a Emanuel Maverakis,^b Shi Bai^c and April M. Kloxin^{id} *^{ad}

An approach for the design of functionalized cyclic peptides is established for use in 3D cell culture and in cell targeting. Sequential orthogonal click reactions, specifically a photoinitiated thiol-ene and strain promoted azide-alkyne cycloaddition, were utilized for peptide cyclization and conjugation relevant for biomaterial and biomedical applications, respectively.

Receptor binding peptides are widely used within the biomaterials and biochemistry communities in the design of *in vitro* cell culture models and targeted therapeutic agents.¹ In particular, the arginine-glycine-aspartate (RGD) peptide sequence broadly has been employed for promoting cell-matrix interactions within two- and three-dimensional (2D and 3D) culture models and for targeting cell surfaces for therapeutic delivery or bioimaging.²⁻⁷ The linear RGD sequence binds a range of different integrins, including $\alpha_v\beta_3$, $\alpha_v\beta_5$, and $\alpha_5\beta_1$ amongst others,² whereas cyclization of RGD has been observed to improve its binding affinity and specificity, especially toward the $\alpha_v\beta_3$ integrin, by mimicking aspects of the helical structure in which RGD is presented within native proteins.⁶⁻⁸ With this increased specificity to $\alpha_v\beta_3$, cyclic RGD has been used for the selective adhesion of specific cell types to substrates in 2D culture *in vitro*^{3,7,9,10} and targeting of therapeutics to tumor cells *in vivo*, which overexpress $\alpha_v\beta_3$.^{5,11} As use of cyclic peptides becomes more prevalent, improved approaches are needed to allow for (1) stable cyclization of RGD, as well as other peptide sequences,¹² and (2) integration

of functional handles for facile incorporation of cyclized peptides within materials for biological applications of interest.

Several approaches have been established for the cyclization of the peptides using chemical or enzymatic ligations, as nicely overviewed in recent reviews.^{13,14} Most commonly, disulfide formation between two cysteines residues or carbodiimide couplings have been utilized.^{6,7} Although these methods are effective for the formation of cyclized RGD, potential drawbacks of these approaches include instability of disulfide bonds in biological systems (*e.g.*, reducing microenvironments like that found in tumors)¹⁵ and amide bonds impacting receptor binding due to the loss of the N- and C-terminus, which can be important in protein binding and downstream signaling events.¹⁶ Toward expanding the toolbox of chemistries available for cyclization, on-resin cyclization has been demonstrated using select click reactions including photoinitiated thiol-ene,¹⁷ thiol-maleimide,¹⁸ and azide-alkyne cycloaddition.¹⁹ Once cyclization is achieved, conjugation of the resulting peptide to material systems of interest also must be considered. Conjugation of cyclized peptides to a variety of systems, including coupling to therapeutics,²⁰ imaging agents,^{20,21} and 2D surfaces,^{3,10} typically has been achieved using either disulfide bond formation or carbodiimide coupling, where one reaction is used for cyclization and the other for conjugation. While these methods have proven useful, inherent instability or cytotoxicity of these coupling chemistries limits their applications. Few simple biocompatible methods exist for formation of cyclized peptides and their subsequent conjugation to biomolecules or culture substrates. We hypothesized that integration of reactive handles for orthogonal click reactions²² into the peptide sequence design would enable sequential cyclization and conjugation for investigations in cell culture and targeting.

Herein, we report a unique approach using orthogonal click reactions for the synthesis of a cyclic RGD peptide with a chemically active functional handle that allows integration within materials systems for 2D and 3D cell culture and cell-labeling applications. Specifically, photoinitiated thiol-ene click chemistry was used to cyclize a linear RGD peptide containing an

^a Department of Chemical and Biomolecular Engineering, University of Delaware, Newark, DE 19716, USA. E-mail: akloxin@udel.edu

^b Department of Dermatology, School of Medicine, University of California Davis, Davis, CA 95616, USA

^c Department of Chemistry and Biochemistry, University of Delaware, Newark, DE 19716, USA

^d Department of Material Science and Engineering, University of Delaware, Newark, DE 19716, USA

† Electronic supplementary information (ESI) available. See DOI: 10.1039/c8cc03218a

‡ These authors contributed equally.

azide functional handle for subsequent conjugation to materials of interest by an azide–alkyne cycloaddition. The utility of this synthetic scheme was demonstrated by the facile incorporation of the peptide into poly(ethylene glycol) (PEG)-based hydrogels for 3D cell culture and attachment to a fluorescent dye for cell targeting. These material systems may prove useful in future studies to investigate the role of $\alpha_v\beta_3$ in cancer progression or to target diagnostic or therapeutic agents to tumor sites for improved treatment strategies. Further, the orthogonal click reaction scheme established here may be easily modified to cyclize and conjugate various peptide motifs for a range of applications.

To synthesize cyclic peptides with an active chemical handle we combined two orthogonal click reactions: (i) a photoinitiated thiol–ene reaction and (ii) an azide–alkyne cycloaddition. The peptide sequence chosen for this demonstration was **cGRGDdvK(alloc)DRK(Az)**, which was inspired by a sequence previously determined to have high binding affinity to $\alpha_v\beta_3$.⁶ D-Cysteine (c) and allyloxycarbonyl (alloc)-protected lysine (K(alloc)) were integrated to flank the binding sequence such that a radically-initiated thiol–ene click reaction could be used to form the cyclized peptide (Fig. 1A). Additionally, an azide functionalized lysine (K(Az)) was incorporated at the C-terminus to impart a functional handle for subsequent conjugation reactions (Fig. 1B and C).

The linear **cGRGDdvK(alloc)DRK(Az)** sequence was successfully synthesized by solid phase peptide synthesis, using an automated peptide synthesizer and standard Fmoc chemistry, purified by reverse phase high performance liquid chromatography (HPLC), and characterized with electrospray ionization (ESI+) mass spectrometry (MS) (Fig. 2A). Initially, the peptide cyclization was attempted on-resin; however, in our hands, this solid-phase cyclization resulted in yields of product that were low and not easily scalable for use in the formation or modification of bulk materials. To improve yield and scalability, a solution-phase approach was adopted: linear RGD functionalized with a pendant thiol, alloc, and azide (5 mM) was dissolved in deionized (DI) water with the photoinitiator lithium acylphosphinate (LAP, 5 mM), and the solution was irradiated with a

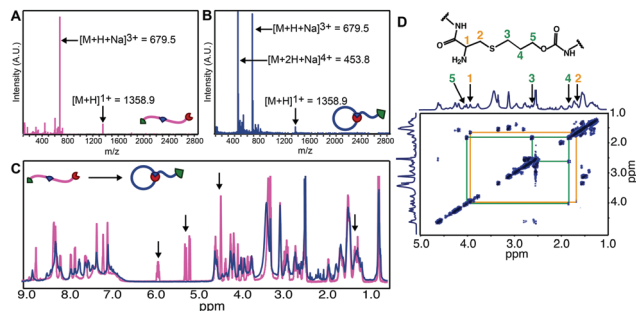


Fig. 2 Characterization of RGD cyclization. No mass gain was observed through ESI+ MS with the transition from the (A) linear peptide to the (B) cyclized peptide. (C) With ^1H NMR, for the linear RGD (pink), the ^1H peaks for the free thiol of the Cys ($\delta = 1.36$ ppm) and the alloc ($\delta = 4.45$, 5.17, 5.26, and 5.9 ppm) were present (arrows) and, upon cyclization (blue), disappeared or shifted. (D) With COSY 2D NMR, the alkyl–sulfide bond formed upon cyclization was observed: orange and green lines indicate the COSY correlations associated with the Cys and the alloc-group attached to the Lys.

low dose of long wavelength UV light for peptide cyclization (20 mW cm^{-2} at 365 nm for 10 minutes). Dilute solution conditions were used to mitigate oligomer formation. After purification by HPLC, this cyclization method afforded product yields of approximately 70%, producing sufficient peptide for use in 3D hydrogel culture systems or conjugation to other molecules of interest. Peptide cyclization was confirmed with a combination of MS and NMR spectroscopy (Fig. 2). With MS, we observed the same molecular weight for the linear peptide sequence and the cyclic peptide sequence, supporting peptide cyclization and retention of the azide during the cyclization process (Fig. 2A and B). Importantly, no higher molecular weights were observed, indicating that no peptide oligomers were present in the purified product. Next, the conversion of the thiol and alloc groups after photoinitiated thiol–ene reaction was confirmed using ^1H NMR (Fig. 2C). Here, we observed the loss of proton signals associated with the Cys ($\delta = 1.36$, 4.06 ppm) and the Lys-alloc ($\delta = 4.45$, 5.17, 5.26, and 5.9 ppm) upon cyclization.

To further confirm the structure of the peptide, 2D NMR was used to observe the alkyl–sulfide bond formed upon successful execution of the thiol–ene reaction. First, the amide peaks associated with the individual amino acids along the peptide backbone were identified using the NOESY cross-peaks of the linear peptide followed by ^1H assignment using a combination of TOCSY and COSY spectra (Fig. S7–S9, ESI[†]). Once the amino acids and their side groups were assigned for the linear peptide, ^1H signals that appeared after the cyclization process were identified, and COSY was used to identify the proton correlations relevant to the formation of the alkyl–sulfide bond (Fig. 2D). Neighboring proton correlations were observed between the alpha proton ($\delta = 3.91$ ppm, peak 1) and the beta proton ($\delta = 1.77$ ppm and $\delta = 1.65$ ppm, peaks 2a and b) for the Cys. The up-field shift observed for the Cys beta protons is speculated to be caused by the ring strain upon cyclization and loss of the proton on the thiol upon bond formation. Similarly, COSY correlations were observed between the three

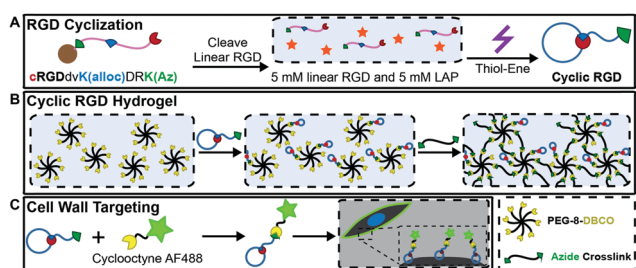


Fig. 1 Synthesis and use of cyclic RGD. (A) Linear RGD was cyclized using a photoinitiated thiol–ene click reaction between the free thiol of the Cys (red) and the alloc protecting group of the Lys (blue). An azide functionalized Lys (green) provided a facile handle for incorporating cyclic RGD into various systems using a SPAAC reaction, including (B) hydrogels for cell culture and (C) conjugation to a fluorophore for cell labeling applications (see Fig. S4 for chemical structures, ESI[†]).

ethyl groups associated with the Lys alloc-protecting group. These peak shifts were identified to be at $\delta = 2.60$ ppm (peak 3), $\delta = 1.80$ ppm (peak 4), and $\delta = 3.99$ (peak 5). No other protons were observed to interact with these protons, which is expected owing to the presence of the sulfur and the amide linkages in the peptide backbone adjacent to the alkyl protons. Taken together, these analyses from ^1H NMR, MS, and 2D NMR support that the thiol-ene reaction was successfully executed to form the desired cyclized product.

To demonstrate the utility of having a cyclic peptide with a functional handle, we first incorporated the cyclic azido-RGD into a poly(ethylene glycol) (PEG)-based hydrogel culture system using strain promoted azide-alkyne cycloaddition (SPAAC) chemistry (Fig. 1B). Cell attachment to the cyclized sequence in 2D culture initially was assessed. Previously, fibroblast, endothelial, and cancer cells have been shown to have good attachment to cyclic RGD presented from surfaces in 2D culture.^{6,7,9} Notably, MDA-MB-231 cells, an aggressive metastatic triple negative breast cancer (TNBC) cell line, highly expresses the $\alpha_v\beta_3$ integrin.²³ Here, we used these MDA-MB-231 cells as a model cell type to examine attachment of cells to hydrogels incorporating the synthesized cyclic RGD. MDA-MB-231s were seeded onto hydrogels with no peptide (negative control), linear RGD (positive control), and cyclic RGD (Fig. 3). The hydrogels were gently rinsed with culture medium 8 hours after seeding to remove any unadhered cells, and cells were subsequently fixed at 24 hours in culture to assess initial cell attachment. MDA-MB-231s exhibited uniform attachment to hydrogel surfaces presenting cyclic RGD (7921 ± 1433 cells cm^{-2}), which was significantly higher than the few cells attached to the no peptide negative control (895 ± 81 cells cm^{-2}) (p -value < 0.05) (Fig. 3A). As expected, MDA-MB-231s also exhibited good attachment to hydrogels presenting linear RGD (8382 ± 1169 cells cm^{-2}), statistically similar to the cyclic RGD condition. Cell morphology also was examined by staining for the cytoskeletal protein F-actin (red) and cell nuclei (blue) (Fig. 3B–D). We observed a rounded morphology of MDA-MB-231s for the few cells attached to the no peptide control and for cells attached to hydrogels presenting linear RGD (Fig. 3B and C). In contrast, MDA-MB-231s seeded onto hydrogels presenting cyclic RGD exhibited a spread and elongated

morphology, which is the typical mesenchymal phenotype of these TNBC cells (Fig. 3D). We hypothesize that the increased affinity and specificity for integrin binding to the cyclic RGD peptide, relative to the linear RGD sequence,²⁴ promoted a more spread morphology at this early culture time point. In sum, these 2D culture studies supported the successful incorporation of pendant peptides within hydrogels and the capacity of the cyclic RGD sequence for promoting cell binding and adhesion after cyclization and immobilization.

Our approach for peptide synthesis and immobilization allows not only presentation from surfaces but also immobilization within hydrogels for 3D cell culture. Indeed, well-defined, 3D culture systems are of continued and growing interest for studying breast cancer amongst other disease and regenerative processes. In particular, within the tumor microenvironment, extracellular matrix interactions are known to be regulated by binding of the $\alpha_v\beta_3$ integrin amongst others.^{23,24} Materials to mimic these interactions could enable the development of improved culture models for studying complex processes, such as the mechanisms of cancer progression, metastasis, and recurrence. Here, to demonstrate the relevance of the azido-cyclic peptide for 3D culture, we encapsulated MDA-MB-231s within hydrogels presenting cyclic RGD and measured cell viability and proliferation over one week in 3D culture (Fig. 4). A live/dead cytotoxicity assay was used to measure the viability of cells (Fig. 4A). Initial cell viability was observed to be typical for encapsulation within PEG-based hydrogels formed using SPAAC chemistry²⁵ (viability $78 \pm 4\%$). After one week in culture, overall cell viability increased to $87 \pm 5\%$, supporting the potential growth and proliferation of cells in these 3D culture environments. Cell viability and proliferation were examined further with measurements of metabolic activity (Fig. 4B) and immunostaining for Ki-67 (Fig. 4C), a nuclear protein associated with cell proliferation that is highly expressed in breast cancer and proliferating breast cancer cells.²⁶ Increased metabolic activity and consistent expression of Ki-67 were observed over 7 days, further supporting proliferation of cells in these 3D cultures. Overall, these studies have demonstrated high viability, growth, and proliferation of human cells in 3D hydrogel-based cultures presenting cyclic RGD. To our knowledge, this is the first demonstration of culturing cells in three dimensions in the presence of a

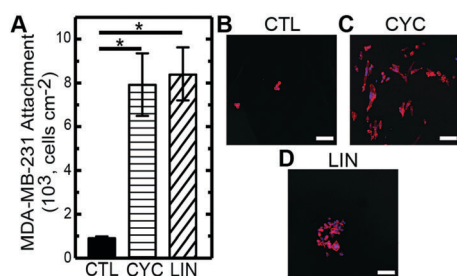


Fig. 3 MDA-MB-231 attachment to cyclic RGD hydrogels. (A) Cell attachment to hydrogels presenting cyclic RGD (CYC) and linear RGD (LIN) (positive control) was significantly higher than without pendant peptide (CTL) (negative control), demonstrating the capacity of the cyclized RGD to promote cell binding and adhesion. Representative images shown for (B) no peptide, (C) cyclic RGD, and (D) linear RGD (F-actin (red), DAPI nuclei (blue)); scale bars, 100 μm (* p -value < 0.05).

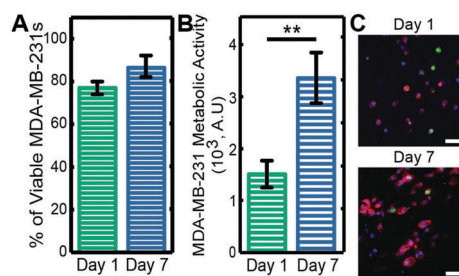


Fig. 4 3D Culture of MDA-MB-231s in hydrogels presenting cyclic RGD. Cells were encapsulated within hydrogels containing cyclic RGD using SPAAC chemistry: (A) good viability was observed with a live/dead cytotoxicity assay, and (B) increased metabolic activity and (C) positive Ki-67 staining further support cell viability and proliferation in these 3D cultures with cyclic RGD (F-actin (red), DAPI (blue), proliferation marker Ki-67 (green)); scale bars, 50 μm (** p -value < 0.01).

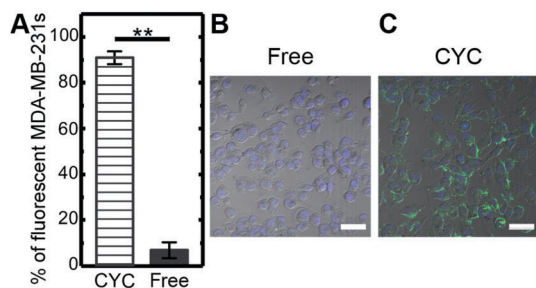


Fig. 5 Fluorescent cyclic RGD labeling of MDA-MB-231 cells. AF488-DIBO was conjugated to the azide handle presented by the cyclic RGD through a SPAAC reaction. (A) Cyclic RGD-AF488 (CYC) labeled a significant portion of the cell population in 2D culture, with few labeled cells observed with the free dye (free, negative control), demonstrating the ability to target the surface of cells by conjugation to cyclic RGD. Representative images of cells incubated with (B) AF-DIBO and (C) cyclic RGD-AF488 for 4 h (scale bars, 50 μm) (** p -value < 0.01).

cyclized peptide, enabled by the orthogonal reactions for cyclization and covalent immobilization. With this approach now established, this 3D culture system could be used in future investigations of disease progression, including the role $\alpha_v\beta_3$ integrin binding, with cyclized RGD, in metastatic disease.²³

Beyond cell culture, targeting of integrins has been utilized for selective delivery of therapeutics and the identification of specific cell types for diagnostic purposes, broadly termed theranostics. In particular, several studies have shown that RGD can be used to target the surface of cancer cells, osteoclasts, and endothelial cells for delivery of therapeutics or for cell-specific fluorescence imaging.⁴ To demonstrate the ability to facilitate modify the azido-RGD peptide synthesized here for such applications, we clicked on an alkyne-functionalized fluorescent tag (Alexa Fluor 488 4-dibenzocyclooctynol, AF488-DIBO) using SPAAC chemistry (Fig. 1C). The resulting fluorescently-tagged cyclic peptide was cultured with MDA-MB-231s. Importantly, cells cultured with the AF488-cyclic RGD exhibited robust labeling of the cell membrane ($91 \pm 3\%$), whereas few cells were observed as labeled when cultured with the free AF488-DIBO (control) ($7 \pm 4\%$) (p -value < 0.01) (Fig. 5). These data demonstrate the potential that the cyclic RGD affords for conjugation with molecules of interest for targeting the cell surface. While not demonstrated here, the azide handle affords the opportunity to use CuAAC chemistry or conversion to other functional handles (e.g., thiols) after cyclization.

In the present study, we demonstrated a facile method to synthesize cyclic RGD peptides with a chemically active handle through orthogonal click reactions. A photoinitiated thiol-ene reaction was utilized for cyclization in solution, which yielded azide-functionalized cyclic peptide on scales relevant for the fabrication of bulk materials. The utility of the azide functionalized cyclic RGD was demonstrated for conjugation to hydrogels and to fluorophores. Overall, the method presented may prove broadly useful in a variety of applications and could be easily modified for a range of systems, including use of different integrin-binding peptide sequences, and for functionalization of surfaces, 3D matrices, or theranostics.

This study was supported by the Delaware COBRE programs, with grants from the NIGMS (P20GM104316 and 5 P30 GM110758-02), the Susan G. Komen Foundation made possible through funding from American Airlines (CCR16377327), the NCI (P30CA093373), the Burroughs Wellcome Fund (1006787), and the CIRM (RN3-06460).

Conflicts of interest

There are no conflicts to declare.

References

- W. Tang and M. L. Becker, *Chem. Soc. Rev.*, 2014, **43**, 7013–7039.
- T. G. Kapp, F. Rechenmacher, S. Neubauer, O. V. Maltsev, E. A. Cavalcanti-Adam, R. Zarka, U. Reuning, J. Notni, H. J. Wester, C. Mas-Moruno, J. Spatz, B. Geiger and H. Kessler, *Sci. Rep.*, 2017, **7**, 39805.
- E. Lieb, M. Hacker, J. Tessmar, L. A. Kunz-Schughart, J. Fiedler, C. Dahmen, U. Hersel, H. Kessler, M. B. Schulz and A. Gopferich, *Biomaterials*, 2005, **26**, 2333–2341.
- K. Miyano, H. Cabral, Y. Miura, Y. Matsumoto, Y. Mochida, H. Kinoh, C. Iwata, O. Nagano, H. Saya, N. Nishiyama, K. Kataoka and T. Yamasoba, *J. Controlled Release*, 2017, **261**, 275–286.
- M. Oba, S. Fukushima, N. Kanayama, K. Aoyagi, N. Nishiyama, H. Koyama and K. Kataoka, *Bioconjugate Chem.*, 2007, **18**, 1415–1423.
- W. Xiao, Y. Wang, E. Y. Lau, J. Luo, N. Yao, C. Shi, L. Meza, H. Tseng, Y. Maeda, P. Kumaresan, R. Liu, F. C. Lightstone, Y. Takada and K. S. Lam, *Mol. Cancer Ther.*, 2010, **9**, 2714–2723.
- J. Zhu, C. Tang, K. Kottke-Marchant and R. E. Marchant, *Bioconjugate Chem.*, 2009, **20**, 333–339.
- J. Wermuth, S. L. Goodman, A. Jonczyk and H. Kessler, *J. Am. Chem. Soc.*, 1997, **119**, 1328–1335.
- S. Petersen, J. M. Alonso, A. Specht, P. Duodu, M. Goeldner and A. del Campo, *Angew. Chem., Int. Ed. Engl.*, 2008, **47**, 3192–3195.
- M. Wirkner, S. Weis, V. San Miguel, M. Alvarez, R. A. Gropeanu, M. Salierno, A. Sartoris, R. E. Unger, C. J. Kirkpatrick and A. del Campo, *ChemBioChem*, 2011, **12**, 2623–2629.
- Z. Guo, X. Zhou, M. Xu, H. Tian, X. Chen and M. Chen, *Biomater. Sci.*, 2017, **5**, 2501–2510.
- A. Roxin and G. Zheng, *Future Med. Chem.*, 2012, **4**, 1601–1618.
- G. K. T. Nguyen and C. T. T. Wong, *J. Biochem. Chem. Sci.*, 2017, **2017**, 1–13.
- A. Zorzi, K. Deyle and C. Heinis, *Curr. Opin. Chem. Biol.*, 2017, **38**, 24–29.
- M. P. Gamesik, M. S. Kasibhatla, S. D. Teeter and O. M. Colvin, *Biomarkers*, 2012, **17**, 671–691.
- G. Marino, U. Eckhard and C. M. Overall, *ACS Chem. Biol.*, 2015, **10**, 1754–1764.
- A. A. Aimetti, R. K. Shoemaker, C. C. Lin and K. S. Anseth, *Chem. Commun.*, 2010, **46**, 4061–4063.
- K. C. Koehler, D. L. Alge, K. S. Anseth and C. N. Bowman, *Int. J. Pept. Res. Ther.*, 2013, **19**, 265–274.
- R. A. Turner, A. G. Oliver and R. S. Lokey, *Org. Lett.*, 2007, **9**, 5011–5014.
- F. Wang, Y. Li, Y. Shen, A. Wang, S. Wang and T. Xie, *Int. J. Mol. Sci.*, 2013, **14**, 13447.
- H. Ma, P. Hao, L. Zhang, C. Ma, P. Yan, R.-F. Wang and C.-L. Zhang, *Eur. Rev. Med. Pharmacol. Sci.*, 2016, **20**, 613–619.
- S. B. Rahane, R. M. Hensarling, B. J. Sparks, C. M. Stafford and D. L. Patton, *J. Mater. Chem.*, 2012, **22**, 932–943.
- S. Takayama, S. Ishi, T. Ikeda, S. Masamura, M. Doi and M. Kitajima, *Anticancer Res.*, 2005, **25**, 79–84.
- D. M. Beauvais, B. J. Ell, A. R. McWhorter and A. C. Rapraeger, *J. Exp. Med.*, 2009, **206**, 691–705.
- C. Guo, H. Kim, E. M. Ovidia, C. M. Mourafetis, M. Yang, W. Chen and A. M. Kloxin, *Acta Biomater.*, 2017, **56**, 80–90.
- M. C. Cheang, S. K. Chia, D. Voduc, D. Gao, S. Leung, J. Snider, M. Watson, S. Davies, P. S. Bernard, J. S. Parker, C. M. Perou, M. J. Ellis and T. O. Nielsen, *J. Natl. Cancer Inst.*, 2009, **101**, 736–750.